(1 blank line)

Dynamics and Control of Clutchless AMTs

Paul D WALKER** Yuhong FANG** Holger ROSER** and Nong ZHANG**
**Centre for Green Energy and Vehicle Innovations, Faculty of Engineering and Information Technology, University of Technology, Sydney
15 Broadway, Ultimo, Australia
E-mail: paul.walker@uts.edu.au

(2 blank lines)

Abstract
Clutchless AMTs (CAMT) have received a large amount of attention recently as they are viewed as compact and economical methods for providing multispeed transmissions to hybrid and electric vehicles. They benefit from not requiring a primary friction clutch for vehicle launch or gear change, instead the increased controllability of electric motors are relied upon for both these functionalities. For vehicle launch the motor can provide maximum torque from rest, enabling simple take-offs. For gear change, synchronisers are opened and motor speed is controlled to achieve the new target speed for component upstream of the gear without the application of friction elements.
This paper presents a detailed control strategy for all stages of gear change in CAMTs so as to demonstrate the impact of the shift process on observable driving performance. This includes torque release and reinstatement as well as speed change in the CAMT during shifting. The complete shift process is then demonstrated on a mathematical model of a CAMT driven electric vehicle, with the impacts on driver observed behavior noted. It shows that both vehicle jerk and the duration of gearshift are influenced by the whole shifting process, not just the speed phase of gear change, as is frequently considered the case.

Key words: Clutch, Automated manual transmission, AMT, powertrain, electric vehicle,

(1 blank line)

1. Introduction

Clutchless automated manual transmissions (CLAMT) have come under scrutiny recently as low cost transmissions systems for use in electric vehicles. Through the integration of multispeed transmissions, higher motor efficiencies and more diverse driving capabilities being sought from electric vehicles additional functionality is achieved through the addition of multiple gear ratios. However such transmission also have drawbacks in the lack of clutch-to-clutch power shifting capabilities.

A typical clutchless AMT powertrain comprises of traction battery and power electronics supplying an electric motor. This electric motor delivers power to the wheels through a stepped automatic transmission. Through varying the selected gear ratio a more diver range of applicable torques and speeds can be achieved at high motor efficiency. Furthermore, as seen by the comparison of Zhou, et al [(1)] and Changenet, et al [(2)], the use of clutchless variants will reduce the transmission system parasitic losses, thereby minimizing the reduction in overall efficiency for the transmission.

A conventional electric vehicle, such as the Nissan Leaf or Mitsubishi iMIEV and early generation Tesla vehicles use a single fixed ratio to deliver load to the road. The BMW i8 uses a two speed AMT to drive the front wheels when the speed is less than 40 km/h. the use of multispeed transmissions for EV applications has been shown to improve drivability of the vehicle through a more diverse application of motor driving torque [(3)] and improve driving range.

As stated earlier, unlike planetary, dual clutch transmissions or even continuously variable transmissions, clutchless AMTs achieve gear change with torque interruption to the wheels during shifting. With the exception of CVTs these transmissions produce power-on gear shifts to minimize the loss of torque to the road[(4)(5)]. This is frequently referred to as the torque hole in the shifting process. This has also been shown to contribute significantly to the quality of the gear shift along with other factors including duration of gearshift and vehicle jerk [(6)].

Clutchless AMTs have been studied in papers such as [(7)(8)]. These papers have typically used either benchtop testing or in vehicle experimentation to study part or all of the shifting process. In [(7)] the speed phase control of the entire gearshift process is studied. This paper provides an improved strategy motor speed control in this phase in particular but does not consider the entire shift process. In [(8)] synchronizer mechanism control is studied to investigate the application for this type of vehicle. The detriment of these papers is that benchtop tests cannot capture the impact on vehicle response, nor do these papers consider the shifting process in its entirety.

The purpose of this paper is to investigate the shift process for clutchless AMTs in its entirety through simulation. To achieve this objective the paper is divided into the following components. Section 2 presents the powertrain system modeling. Including (1) equivalent DC motor model, (2) powertrain system model, and in (3) a simplified synchronizer mechanism model. Section 3 contains a detailed development of the control algorithm an strategy studied for gear shift control of the CLAMT. Section 4 presents the simulation results for the study, and section 5 presents the concluding remakes.

2. Powertrain system modeling

The CLAMT powertrain model is divided into four component systems, (1) electric machine, (2) multi-body powertrain model, (3) simplified synchronizer mechanism model, and (4) vehicle torque model. These models are presented in this section.

2.1 Equivalent motor model

To simplify the system model a DC equivalent motor model is used to represent the prime mover. This reduces the three phase permanent magnet motor to a simple two degree of freedom model, and allows direct control of input voltage without consideration of power electronics for these simulations. The complexity of simulating power electronics is eliminated and the direct voltage control of the motor is now possible. The simplified DC circuit for the model is shown in Figure 1.

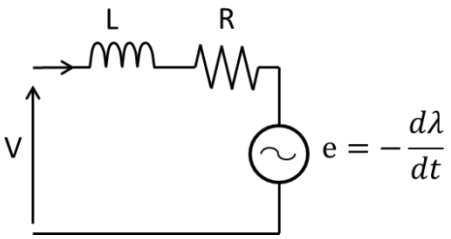

Figure 1: DC equivalent circuit model

The differential equation for the electric circuit is defined as:

$$L\dot{I_{EM}} = K_e\dot{\theta_1} - RI_{EM} + V \quad (1)$$

where IEM is the line current, L is the line inductance, Ke is the back emf constant, R is the line resistance, and V is line voltage.

The electromagnetic torque produced in the EM is defined as follows:

$$T_{EM} = K_T I_{EM} \quad (2)$$

where K_T is the torque constant and T_{EM} is the electromagnetic torque. These two equations represent the electrical component of the model equations of motion, and should be considered in conjunction with the equations of motion presented

2.2 Powertrain system model

The powertrain system is modeled as a multi-body dynamic system model, using the layout shown in Figure A below. This model includes motor rotor, coupled to the equations in Section 2.1, gear set for the transmission, final drive, wheels and equivalent vehicle inertia. The multi-body model is shown in Figure 2 for reference, and equations of motion derived in Equations 5 to 13. For the model J_1 represents the motor rotor and is coupled to the DC motor model and equations of motion, J_{2a} is the synchronizer equivalent inertia, J_{eq} is the equivalent transmission inertia, J_4 and J_6 represent wheel hubs and J_5 and J_7 are the equivalent vehicle inertias.

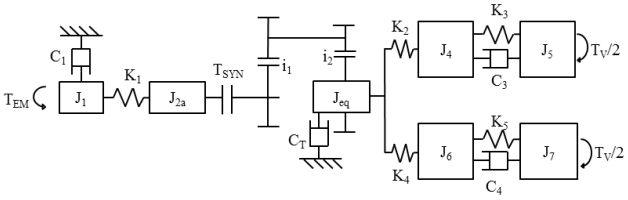

Figure 2: Multi-body Powertrain Model

The equations of motion for each degree of freedom are shown below for reference:

$$J_1\ddot{\theta}_1 = T_{EM} - C_1\dot{\theta}_1 - K_1(\theta_2 - \theta_1) + C_1(\dot{\theta}_2 - \dot{\theta}_1) \quad (5)$$

$$J_2\ddot{\theta}_2 = -K_1(\theta_2 - \theta_1) - C_1(\dot{\theta}_2 - \dot{\theta}_1) - T_{SYN} \quad (6)$$

$$J_{eq}\ddot{\theta}_3 = i_1 i_2 T_{SYN} - C_T\dot{\theta}_3 + K_2(\theta_4 - \theta_3) + C_2(\dot{\theta}_4 - \dot{\theta}_3) + K_4(\theta_6 - \theta_3) + C_4(\dot{\theta}_6 - \dot{\theta}_3) \quad (7)$$

$$J_4\ddot{\theta}_4 = -K_2(\theta_4 - \theta_3) - C_2(\dot{\theta}_4 - \dot{\theta}_3) + K_3(\theta_5 - \theta_4) + C_3(\dot{\theta}_5 - \dot{\theta}_5) \quad (8)$$

$$J_5\ddot{\theta}_5 = -K_3(\theta_5 - \theta_4) - C_3(\dot{\theta}_5 - \dot{\theta}_5) - T_V/2 \quad (9)$$

$$J_6\ddot{\theta}_6 = -K_4(\theta_6 - \theta_3) - C_4(\dot{\theta}_6 - \dot{\theta}_3) + K_5(\theta_7 - \theta_6) + C_5(\dot{\theta}_7 - \dot{\theta}_6) \quad (10)$$

$$J_5\ddot{\theta}_5 = -K_5(\theta_7 - \theta_6) - C_5(\dot{\theta}_7 - \dot{\theta}_6) - T_V/2 \quad (11)$$

where J_n represents the inertia of any given powertrain element, C_n represents damping coefficients, K_n represents stiffness elements, θ represents rotational displacement, and its two time dirivatives represent velocity and acceleration. n represents the nth element of the powertrain model in Figure 2. i represents the gear ratios, subscript 1 represents any of the given transmission ratios and 2 is the final drive ratio. For the closed transmission condition with any of the gears engaged Equations 5 to 7 are reduced as follows:

$$J_1\ddot{\theta}_1 = T_{EM} - C_1\dot{\theta}_1 - K_1(i_1 i_2\theta_3 - \theta_1) + C_1\left(i_1 i_2\dot{\theta}_3 - \dot{\theta}_1\right) \quad (12)$$

$$\left(J_{eq} + i_1^2 i_2^2 J_2\right)\ddot{\theta}_3 = -i_1 i_2 K_1(i_1 i_2\theta_3 - \theta_1) - i_1 i_2 C_1\left(i_1 i_2\dot{\theta}_3 - \dot{\theta}_1\right) - C_T\dot{\theta}_3 + K_2(\theta_4 - \theta_3) + C_2\left(\dot{\theta}_4 - \dot{\theta}_3\right) + K_4(\theta_6 - \theta_3) + C_4\left(\dot{\theta}_6 - \dot{\theta}_3\right) \quad (13)$$

2.3 Simplified synchronizer mechanism model

Detailed synchronizer mechanism modeling has been previously conducted in papers such as Walker[9] and Lovas[11]. These papers have detailed intricate models that capture multiple stages in the engagement process. For the purposes of this paper it is assumed that the mechanism will successfully engage under each actuating instance, therefore it is possible to simplify the model to the main actuating process: speed synchronization. This phase is critical for this model as it ensures speed matching is completed successfully and allows the engagement process to continue such that the dog clutch will successfully lock the mechanism.

The model is based on the different stages of engagement is described as follows:

First free fly – here the sleeve moves from the neutral position to contact with the cone clutch. In this model it is simulated using a spring-damper element to capture delay in actuation

Speed synchronisation – here any residual relative motion between engaging synchroniser elements is eliminated through the energising of the cone clutch. The cone clutch torque is described as follows:

$$T_{SYN} = \frac{\mu_D R_C P}{sin\alpha} \quad (14)$$

Where T_{SYN} is the cone torque, μ_D is the dynamic friction coefficient, R_C is the mean cone radius and α is the cone angle.

Ring release and hub engagement – For these two stages of engagement spring damper elements are again used to simulate the engagement process and ensure an appropriate time delay between actuation and completion of engagement. Upon the complete displacement of the synchroniser sleeve it is assumed that the mechanism is locked and the shifting process can continue to completions.

It is recognized that whilst this does not strictly simulate the engagement process for a synchronizer mechanism, as studied in Walker[9][10]. The process is representative of the actual delays present in synchronizer engagement and is sufficient for this paper. Furthermore, it must be assumed that engagement is always successful for this strategy to be appropriate.

2.4 Vehicle torque model

The vehicle resistance torque is defined from a combination of road grade, rolling resistance of the vehicle, and aerodynamic drag as follows:

$$T_V = \left(C_R M_v g cos\emptyset + M_V g sin\emptyset + \tfrac{1}{2} C_D \rho A_V V_V^2\right) r_t \quad (15)$$

where C_R is rolling resistance, g is gravity, ϕ is road incline angle, C_D is drag coefficient, ρ is air density, A_V is frontal area, V_V is linear vehicle speed.

3. Gear shift control strategy

Control of clutchless AMTs requires a combination of speed and torque control strategies. For a conventional AMT the primary clutch is released prior to gear change. This has the effect of isolating both the transmission and remainder of the driveline from the engine during the shift process. This has the effect of significantly reducing the load on the synchronizer during gear selection.

The combined torque-speed control of the gear change process in clutchless AMTs is shown in Figure YY. It includes (1) motor torque reduction, (2) synchronizer disengagement, (3) motor speed control (4) synchronizer engagement, and (5) torque re-instatement of the motor. For stages (2) and (4) the synchronizer mechanism is released and engaged according to Section 2.2. For the motor torque and speed control phases of gear change closed loop control of either motor torque for stages (1) and (5) or relative motor speed for stage (3) is utilized with predetermined torque or slip speed profiles.

Motor torque control is the predominant control method during normal operation and during gear shift for the CLAMT powertrain system in this study. During normal operation torque is a command input from the driver. During synchronizer release and engagement and during inertia phase control the reference torque is set to zero.

During torque release and reinstatement a modified bump function is used to define the profile for closed loop motor control.

$$T_{P1} = Ae^{\frac{-1}{1-x^2}} \quad (16)$$

where A is the scaling factor to equate the bump amplitude to the input torque at the initiation of shifting, and x = $(t_0\text{-}t)/t_D$. Here t_0 is time at initiation of profiled control and t_D is the desired duration of the particular phase. This allows for the control of the duration of torque release and reinstatement. For torque reinstatement the modified function is used as follows, where B is the target torque at the completion of shifting:

$$T_{P2} = B - Ae^{\frac{-1}{1-x^2}} \quad (17)$$

Slip speed control is utilized for the synchronization of synchronizer mechanism slip speeds. Through this strategy a speed profile based on the bump function is again used to achieve the desired new speed. This is as follows:

$$\dot{\theta}_P = i_T i_2 \dot{\theta}_3 + i_A i_2 \dot{\theta}_{3,0} e^{\frac{-1}{1-x^2}} \quad (18)$$

Where subscripts A and T are for actual and target gear, respectively, and the 0 subscript on the speed is for the speed at the beginning of the inertia phase. Again, the bump function is used to control the duration of shifting so that its impact can be studied in this paper.

The use of the equivalent DC motor model allows for the direct control of motor functionality through variation of input voltage. Two proportional-integral-derivative control loops are employed to enable closed loop speed and torque control of the powertrain. Torque control is used for the primary driving input for the system under normal operation and motor speed control is utilized for the inertia phase of gear shift. The loop arrangement is shown in Figure 4 for reference. With the desired motor torque the desired input, under either normal driving conditions or during shifting.

3. Simulations

Simulations for this study focus on the impact of a series of up and down shifts on the vehicle acceleration and jerk. For the purpose of these simulations the model values are taken as being typical data and are presented at the end of this section in Table 1. For simulations a constant input torque of 200Nm is used as a demand input and up shifts through gear ratios selected based on an earlier study in Walker[12]. Using the same demand torque a series of downshifts are then performed to compare results. This is then followed with comparative simulations using a lower time constant for Equations 16 to 18 for a shorter shift time, followed by an extended shift duration with the impact on vehicle transients studied.

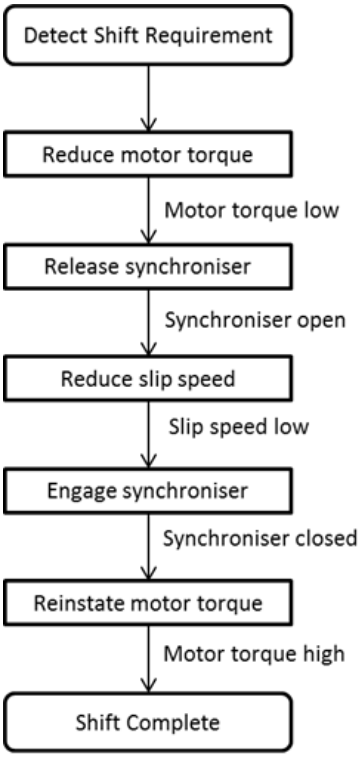

Figure 3: CLAMT shifting strategy.

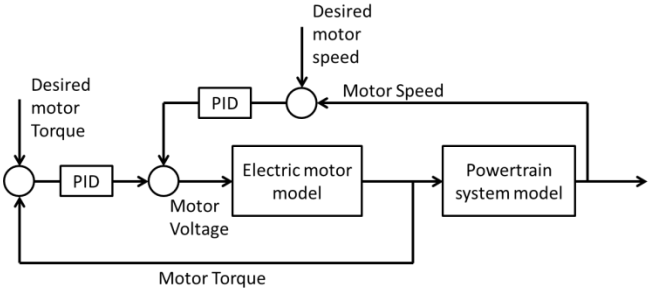

Figure 4: Combined torque-speed control loops

The first series of simulation results are presented in Figure 5 for a t_D of 200ms. This time constant will influence the duration of the entire shift as well as torque release and reinstatement along with the speed synchronization process. It is arbitrary, but set with the goal of maintaining a shift time of less than one second.

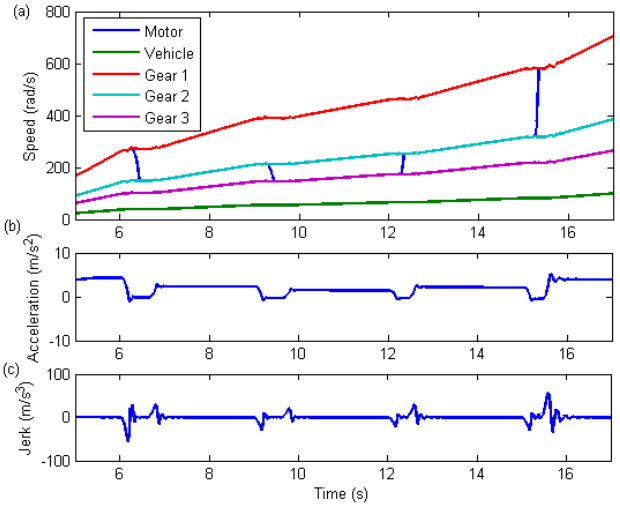

Figure 5: Up and down shift transients for clutchless AMT powertrain for a 200ms stage duration at 200Nm motor torque (a) system speeds, (b) vehicle longitudinal acceleration, and (c) vehicle longitudinal jerk

The previous simulation is repeated in Figure 6 using a tD of 20ms. This time is chosen to represent a minimal duration of shifting, and the impact on vehicle response. These results demonstrate that vehicle transients peak as the speed of torque release is increased. However, minimizing the speed phase of shifting does not impact on vehicle response. Therefore it can be minimized in such a way to reduce the shift duration.

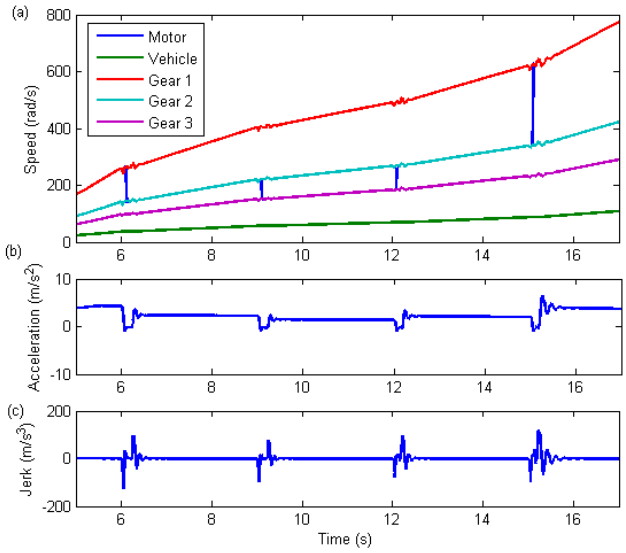

Figure 6: Up and down shift transients for clutchless AMT powertrain for a 20ms stage duration at 200Nm motor torque (a) system speeds, (b) vehicle longitudinal acceleration, and (c) vehicle longitudinal jerk

For the final series of simulations extends tD to 400ms. In these simulations the duration of gear shift is maximized, and is observed in the longer periods of vehicle deceleration. However, vehicle jerk is significantly reduced, peaking at approximately $30m/s^3$. This is obviously a more desirable response for the system. Consequently, it is observed that the balanced control for reducing vehicle jerk at the cost of longer deceleration periods requiring a balanced shift algorithm.

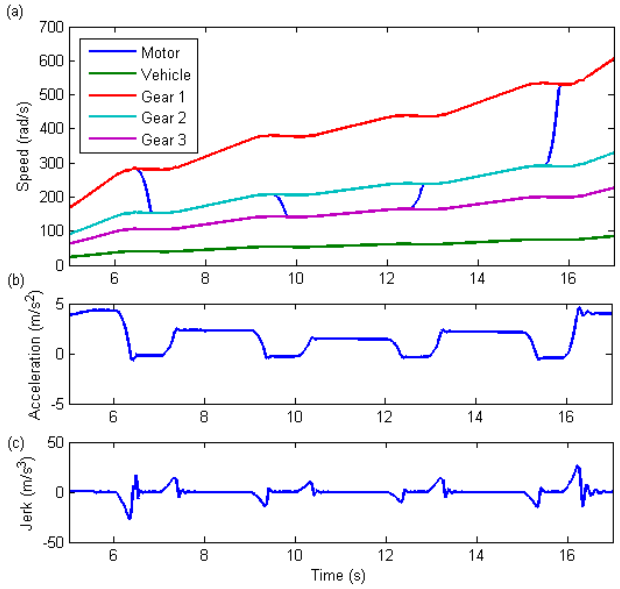

Figure 7: Up and down shift transients for clutchless AMT powertrain for a 400ms stage duration at 200Nm motor torque (a) system speeds, (b) vehicle longitudinal acceleration, and (c) vehicle longitudinal jerk

5. Conclusion

The purpose of this paper is the presentation of a detailed model of clutchless automated manual transmission systems for the purpose of investigating the shift response of the system. In doing so the different stages of gearshift have been identified and a shift control algorithm presented that is inclusive of the different shift stages. Using vehicle acceleration and jerk as measures of shift performance several outcomes have been identified. Particularly:

1. The duration of motor torque release and reinstatement actives influences the peak accelerations and jerks observed during shifting.
2. The duration of the speed phase of shifting only impacts on the total gear change time. It does not influence the quality of gear shift
3. Motor speed control can be effectively used to minimize the speed phase and it may therefore be possible to remove and friction elements

from the transmission, improving transmission efficiency.

6. References

(1) Zhou, Xingxing, Paul Walker, Nong Zhang, Bo Zhu, and Jiageng Ruan. "Numerical and experimental investigation of drag torque in a two-speed dual clutch transmission." Mechanism and Machine Theory 79 (2014): 46-63.

(2) Changenet, C., Oviedo-Marlot, X. and Velex, P. Power loss predictions in geared transmissions using thermal networks-application to a six speed manual gearbox. Journal of Mechanical Design, 128, 2006 pp. 618-625.

(3) Walker, PD., Abdul Rahman, S, Zhu, B, Zhang, N Modelling, Simulations, and Optimisation of Electric Vehicles for Analysis of Transmission Ratio Selection Advances in Mechanical Engineering, Volume 5, 2013. pp. 340435.

(4) Crowther, A. R., Singh, R., Zhang, N., Chapman, C. Impulsive response of an automated transmission system with multiple clearances: formulation, simulation, and experiment, Journal of Sound and Vibration, 306 (2007), 444-466.

(5) Zhang Y, Chen X, Zhang X, Jiang H, Tobler W, Dynamic Modelling and Simulation of a Dual-Clutch Automated Lay-Shaft Transmission, Journal of Mechanical Design, 127 (2005), 302-307.

(6) Zhu, B, Zhang, N, Walker, PD, Zhan, W, Zhou, X, Ruan, J "Two-Speed DCT Electric Powertrain Shifting Control and Rig Testing" Advances in Mechanical Engineering, Dec 2013; vol. 5: pp. 323917

(7) Zhu, X., Zhang, H., Xi, J., Wang, J., & Fang, Z. (2014). Robust speed synchronization control for clutchless automated manual transmission systems in electric vehicles. Proceedings of the Institution of Mechanical Engineers, Part D: Journal of Automobile Engineering, 0954407014546431.

(8) Tseng, C. Y., & Yu, C. H. (2015). Advanced shifting control of synchronizer mechanisms for clutchless automatic manual transmission in an electric vehicle. Mechanism and Machine Theory, 84, 37-56.

(9) Walker, PD; Zhang, N; 2011 "Parameter study of synchroniser mechanisms applied to Dual Clutch Transmissions", International Journal of Powertrains, 1(2), pp. 198-220.

(10) Walker, PD; Zhang, N; 2012 "Engagement and control of synchroniser mechanisms in dual clutch transmissions" Mechanical Systems and Signal Processing, 26, pp. 320-332.

(11) L. Lovas, D. Play, J. Marialigeti, J. Rigal, Mechanical beaviour simulation for synchromesh mechanism improvements, IMechE Part D: Journal of Automobile Engineering 220 (2006) 919–945.

(12) Walker, P., Roser, H., Zhang, N., and Fang, Y., "Comparison of Powertrain System Configurations for Electric Passenger Vehicles," SAE Technical Paper 2015-01-0052.

Acknowledgements

The authors would like to gratefully acknowledge the support of the AutoCRC and Changzhou New Energy Vehicle Academy for their support on this project. We also acknowledge funding provided by the Australian Research Council through DP150102751